R = radius of cell, ft
z = distance from the cake surface, ft
σ_r = horizontal component of stress, lb_f/ft^2
σ_z = vertical component of stress, lb_f/ft^2

LITERATURE CITED

1. Delaplaine, J. W., *AIChE J.*, **2**, 127 (1956).
2. Glastonbury, B. E., and P. G. Bratel, *Trans. Inst. Chem. Engrs., (London)* **44T**, 128 (1966).
3. Grace, H. P., *Chem. Eng. Progr.*, **49**, 303, 367 (1953).
4. Haynes, S. Jr., Ph.D. thesis, Univ. of Houston, Texas (1966).
5. Ingmanson, W. L., *Chem. Eng. Progr.*, **49**, 577 (1953).
6. Jaky, J., Proc. of Second Intern. Conf. on Soil Mech. Foundation Eng., **1**, 103 (1948).
7. Jenkin, C. F., *Proc. Royal Soc. (London)*, **A131**, 53 (1931).
8. Kottwitz, F. A., and D. R. Boylan, *AIChE J.*, **3**, 433 (1958).
9. Lu, W. M., Ph.D. thesis, Univ. of Houston, Texas (1968).
10. Lu, W. M., F. M. Tiller, Fan-Bill Cheng, and Chin-Tu Chien, *J. Chin. Inst. Chem. Engr.*, **1**, 45 (1970).
11. Okamura, S., and M. Shirato, *Chem. Eng. (Japan)*, **18**, 59, 358 (1954); **19**, 104, 111 (1955).
12. Rawling, F. L. Jr., Ph.D. thesis, Iowa State Univ., Ames (1964).
13. Rowe, P. W., *Proc. Royal Soc. (London)*, **A269**, 500 (1962).
14. Ruth, B. F., *Ind. Eng. Chem.*, **38**, 564 (1946).
15. Sambuichi, M., Ph.D. thesis, Nagoya Univ., Japan (1967).
16. Sawamoto, K., M.S. thesis, Nagoya Univ., Japan (1967).
17. Shirato, M., T. Aragaki, R. Mori, and K. Sawamoto, *J. Chem. Engr. Japan*, **1**, 86 (1968).
18. Tiller, F. M., S. Haynes, and Wei-Ming Lu, *AIChE J.*, **18**, 13 (1972).
19. Tschebotarioff, G. P., and J. D. Welch, Proc. of Second Intern. Conf. Soil Mech. Foundation Eng., **7**, 135 (1948).

Manuscript received December 17, 1970; revision received January 4, 1972; paper accepted January 6, 1972.

The Dynamics of a Packed Gas Absorber by the Pulse Response Technique

NORIHIKO SAKATA and JOHN W. PRADOS

Department of Chemical and Metallurgical Engineering
The University of Tennessee, Knoxville, Tennessee 37916

The dynamic response of a packed gas absorber to inlet gas composition changes was investigated by the pulse response technique for the case where absorption was accompanied by pseudo first-order irreversible chemical reaction.

The solute-carrier-solvent system was carbon dioxide-air-0.07 normal aqueous sodium hydroxide solution. The column used was 6.5 in. I.D. Plexiglass packed to a height of 6.15 ft. with either ¼-in. Raschig rings or ¾-in. Berl Saddles. Gas flow rates ranged from 1.5 to 10 lb.-moles/hr./sq.ft. and liquid flow rates ranged from 0 to 200 lb.-moles/hr./sq.ft. A pulse of carbon dioxide was injected into the inlet air stream and monitored as it entered the packed section. The outlet gas and liquid phase concentrations were continuously monitored as the resulting pulses left the packed section. The pulse response data were reduced to frequency response by digital computer calculations. Reliable data could be obtained over the frequency range 0 to 5 radians/second.

The experimental results were compared with theoretical predictions from the slug flow, axial diffusion, and mixing cell models. Both the mixing cell model and the axial diffusion model satisfactorily predicted the experimental frequency responses over the entire frequency range covered. The slug flow model was found unsatisfactory for predicting gas-phase amplitude ratios at high frequencies, where axial mixing affected the amplitude ratios. Gas-phase particle Peclet numbers and overall mass transfer coefficients based on the gas-phase driving force determined in the present absorption system were in reasonable agreement with the values reported in the literature.

The rational design of process control systems, the development through simulation of effective plant start-up procedures, and the proper sizing of equipment for unsteady state applications require valid mathematical models describing the dynamic behavior of each unit in the process system. Over the past fifteen years a number of papers

dealing with process equipment dynamics have appeared; however, almost none have provided experimental dynamic response measurements for the important unit operation of gas absorption in packed columns, and the use of these data to validate mathematical models of gas absorber dynamics.

Work in this area was first reported by Gray and Prados (9) who investigated the dynamics of absorption of carbon dioxide from an air stream into water in a packed column by the frequency response technique. They determined the response of exit gas composition to sinusoidal inlet gas composition changes and compared the results with theoretical predictions from three mathematical models. Agreement between theory and experiment was fair and sufficiently encouraging that work was continued to develop more refined experimental techniques and to extend the studies to systems providing much higher absorption rates at atmospheric pressure than were obtainable with air-carbon dioxide-water.

The present work utilizes the pulse response technique, deals with high mass transfer rate operation, and includes the measurement of changes in composition of the outlet liquid as well as the outlet gas.

Chemical absorption of carbon dioxide from an air stream into aqueous sodium hydroxide solutions was adopted since this system proved to be inexpensive, provided high mass transfer rates, and offered a convenient method of analysis of gas and liquid composition changes.

Experimental frequency responses were determined by the pulse technique following the methods presented by Hougen and Walsh (*11*) and by Clements and Schnelle (*4*).

THEORETICAL DEVELOPMENTS

Three models which differ only in the manner of describing the flow behavior along the column were used to calculate the theoretical frequency response for the absorption process. They are referred to as the slug flow, mixing cell, and axial diffusion models. In each model, mass transfer was described by the following rate equation based on diffusion and simultaneous slow pseudo first-order reaction as presented by Hatta (*10*)

$$Ra = K_G a\, y \tag{1}$$

where

$$\frac{1}{K_G a} = \frac{1}{k_G a} + \frac{m}{\beta k_L a}. \tag{2}$$

This equation was chosen since the theoretical concept of the reaction factor β is widely used and supported experimentally, and literature values on $K_G a$ are available.

It should be noted that β is a factor by which the liquid-phase mass transfer coefficient is enhanced due to chemical reaction. Its magnitude depends upon the concentration of hydroxyl ion in the liquid phase, and this functional dependence, as predicted by Hatta's analysis, is shown in the Notation. In the present work, however, β is treated as a constant; under the experimental conditions employed changes in hydroxyl ion concentration were usually less than 10% of the value in the liquid entering the column, leading to variations in β of less than 5%.

Because the absorption may be considered irreversible and the liquid remains unsaturated at the composition levels employed, the mathematical models are simpler to use than those presented by Gray and Prados (9) for physical absorption. In the present work, the gas-phase material balance contains only gas-phase compositions and may be solved independently of the liquid-phase balance.

Slug Flow Model

For the slug flow model the conservation of solute component in the gas and liquid phases for an incremental packing height dz leads to the following equations under the assumptions that holdups and flow rates are constant:

$$h_G \frac{\partial y}{\partial t} = -G \frac{\partial y}{\partial z} - Ra \tag{3}$$

$$h_L \frac{\partial x}{\partial t} = L \frac{\partial x}{\partial z} + Ra, \tag{4}$$

with the limiting conditions

$$y(z, 0) = 0; \quad x(z, 0) = 0; \quad y(0, t) = y_0;$$
$$x(Z, t) = x_Z = 0. \tag{5}$$

For this absorption system, x is mole fraction of CO_3^{--} in liquid phase, which is equivalent to an imaginary mole fraction of carbon dioxide in the liquid phase.

Equations (3) and (4) are converted into ordinary differential equations by application of the Laplace transformation with respect to time, and the resulting equations are solved simultaneously with the transformed boundary conditions to yield the transfer functions for gas and liquid phases.

$$\frac{\bar{y}_Z}{\bar{y}_0} = e^{-N}\, e^{-\theta_G s} \tag{6}$$

$$\frac{\bar{x}_0}{\bar{y}_0} = \frac{1}{\phi} \frac{1 - e^{-N}\, e^{-\theta_T s}}{1 + \dfrac{\theta_T}{N} s} \tag{7}$$

The frequency responses are obtained by substituting $i\omega$ for s in Equations (6) and (7). The magnitude and argument of the resulting complex number are the amplitude ratio and the phase shift, respectively; they were calculated directly by a digital computer program written in Fortran IV and making use of complex arithmetic operations.

Mixing Cell Model

For the mixing cell model, in which longitudinal mixing is accounted for by assuming the column to act as a series of finite perfectly mixed cells, the conservation of the liquid and gas components in the jth cell with height Δz yields

$$\frac{\theta_G}{J} \frac{dy_j}{dt} = y_{j-1} - y_j - \frac{N}{J} y_j \tag{8}$$

$$\frac{\theta_L}{J} \frac{dx_j}{dt} = x_{j+1} - x_j + \frac{1}{\phi} \frac{N}{J} y_j. \tag{9}$$

The above equations are converted into difference equations by Laplace transformation and the resulting equations are solved with the transformed boundary conditions $\bar{y}_j = \bar{y}_0$ at $j = 0$ and $\bar{x}_j = 0$ at $j = J + 1$ to give the system transfer functions

$$\frac{\bar{y}_J}{\bar{y}_0} = \frac{1}{p^J} \tag{10}$$

$$\frac{\bar{x}_0}{\bar{y}_0} = \frac{1}{\phi} \frac{N}{J} \frac{1}{pq - 1} \left[1 - \frac{1}{(pq)^J} \right] \tag{11}$$

where

$$p = 1 + \frac{N}{J} + \frac{\theta_G}{J} s$$

$$q = 1 + \frac{\theta_L}{J} s \tag{12}$$

The amplitude ratio and phase shift are calculated as with the slug flow model.

Axial Diffusion Model

In the axial diffusion model, mixing along the column is described by an expression of the form of Fick's law

$$h_G \frac{\partial y}{\partial t} = -G \frac{\partial y}{\partial z} + h_G E_G \frac{\partial^2 y}{\partial z^2} - K_G a y \tag{13}$$

$$h_L \frac{\partial x}{\partial t} = L \frac{\partial x}{\partial z} + h_L E_L \frac{\partial^2 x}{\partial z^2} + K_G a y \tag{14}$$

The above material balance equations are Laplace transformed and are subjected to the following transformed boundary conditions, which presume composition discontinuities at the inlet boundaries, as derived by Danckwerts (5).

$$\left.\begin{array}{l} \text{at } z = 0 \\ \left\{\begin{array}{ll} \bar{y}_0 = \bar{y}(0^+) - \dfrac{Z}{Pe_G} \dfrac{d\bar{y}}{dz}\Big|_{0^+} & \text{for gas phase} \\ \dfrac{d\bar{x}}{dz}\Big|_{0^+} = 0, \quad \bar{x}_0 = \bar{x}(0) & \text{for liquid phase} \end{array}\right. \\ \text{at } z = Z \\ \left\{\begin{array}{ll} \dfrac{d\bar{y}}{dz}\Big|_{Z^-} = 0 & \text{for gas phase} \\ \bar{x}_Z = \bar{x}(Z^-) + \dfrac{Z}{Pe_L} \dfrac{d\bar{x}}{dz}\Big|_{Z^-} = 0 & \text{for liquid phase} \end{array}\right. \end{array}\right\} \tag{15}$$

The solutions lead to the following transfer functions.

$$\frac{\bar{y}_Z}{\bar{y}_0} = b_1 e^{m_1} + b_2 e^{m_2} \tag{16}$$

$$\frac{\bar{x}_0}{\bar{y}_0} = \frac{1}{\phi} N [(c_1 - c_2) - (Ab_1 - Bb_2)]. \tag{17}$$

An analogous transfer function and the resulting frequency response to that for the gas phase have been obtained by Fan and Ahn (8) for a tubular reactor with a first order chemical reaction.

More detailed developments of all the transfer functions appearing in this section are presented by Sakata (15).

EXPERIMENT

Equipment

The dynamic gas absorption experiment was conducted in a 6.5-in. I.D. Plexiglas pipe packed with either ¼-in. Raschig rings or ¾-in. Berl saddles to a height of 6.15 ft. The column top and bottom sections were carefully designed by Byington (3) to prevent the two phases from contacting each other below and above the packed section and to permit monitoring of the composition as close as possible to the ends of the packed section. This eliminated the necessity of separate treatment of the column end sections in the calculation of experimental dynamic response (9).

Figure 1 is a schematic diagram of the air, carbon dioxide, and liquid flow systems. Air was forced into the column by a positive displacement blower which could provide air flows of 0 ~ 15 cu.ft./min. The air flow rate was adjusted by a variable speed drive on the blower and a by-pass arrangement and was measured with a rotameter. Just upstream from the column inlet, the temperature and static pressure of the air stream were measured.

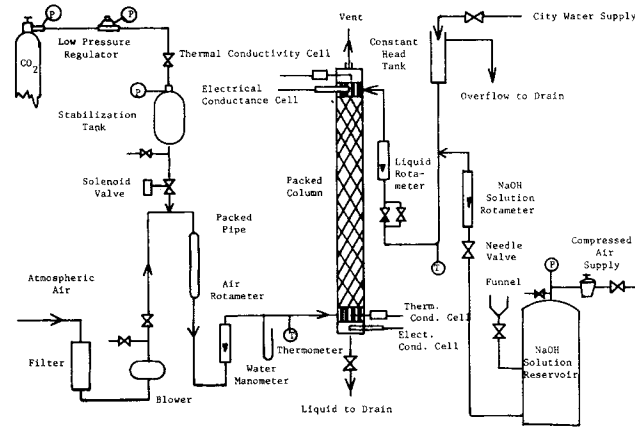

Fig. 1. Schematic diagram of column flow system.

Carbon dioxide was fed from a cylinder to a 2,100 cu. in. stabilizer tank. The pressure in the tank was adjusted by a low pressure regulator in accordance with the air flow rate. An inlet gas pulse was formed by injecting CO_2 from the stabilization tank through a solenoid valve into the air stream; the CO_2 was thoroughly mixed with the air stream in a 1.5-ft. section of 2-in. pipe packed with ¼-in. Raschig rings before entering the column. The solenoid valve was controlled by a cam-operated microswitch. The cam was driven by a synchronous motor and could be adjusted to allow the valve to remain open for the desired period; the valve was held open for 0.70 sec. in this investigation.

A 0.07 N aqueous NaOH solution was fed to the top of the column either directly from the NaOH solution reservoir when the liquid flow rate was small, or by mixing concentrated NaOH solution from the reservoir with tap water continuously in a fixed ratio. The tap water was supplied from a constant head tank by gravity. The NaOH reservoir was pressurized to 4 ~ 8 lb./sq.in.gauge by compressed air to force the solution to the top of the column at a rate controlled by a needle valve and measured by a rotameter. The total liquid flow rate to the column was adjusted by valves and measured by a rotameter.

The concentration of carbon dioxide in the inlet and outlet gas streams was measured by thermal conductivity cells employing thermistors as the sensing elements in a Wheatstone bridge. The cells used in this investigation were designed by Byington (3) and based on the original design by Gray (9). A complete description of the cell design and development is given by Gray (9).

The measurement of the change in NaOH concentration in the liquid due to the CO_2 absorption was accomplished by electrical conductance measurements. A reference cell was placed in the incoming liquid above the packing and a sampling cell was mounted beneath the packing. The change in liquid conductance at the sampling cell relative to the conductance at the reference cell, which was directly related to the liquid composition, was measured and recorded using a Wheatstone bridge circuit. A detailed description of the cell assembly and the method of determining the extent of absorption is presented by Sakata (15).

Procedure

Prior to operation of the system the flowmeters, the thermal conductivity cells, and electrical conductance cells were calibrated. The packing porosity, the liquid static holdup, and the liquid operating holdup were determined. The calibration and holdup measurement details are given by Sakata (15).

The concentration of aqueous sodium hydroxide solution to be used was determined by trial and error. Concentrations tested were 0.04, 0.05, 0.06, 0.07, 0.08, 0.10, 0.15, and 0.20 N.

The concentration of 0.07 N was chosen since it gave stable and sensitive electrical conductivity cell operation, and the mass transfer rates at this concentration were sufficiently high to exert a significant influence on the packed column dynamics.

An aqueous sodium hydroxide solution of known concentration was prepared in the NaOH solution tank and the tank was pressurized. The column packing was wetted thoroughly prior to all gas absorption runs. For the runs without absorption (no liquid flow) the packing was dried completely by blowing air through the column. The pressure of the carbon dioxide stabilizer tank was adjusted to the desired value. The gas and liquid flow rates were set to their desired values. After a steady state was reached, a sample of the liquid was taken to determine its NaOH concentration. Then the microswitch timing cam was started to inject a pulse of carbon dioxide into the air stream through the solenoid valve. The peak carbon dioxide concentration in the inlet pulse was kept approximately constant at around 11% throughout all the runs. Input and output gas phase carbon dioxide concentrations and output liquid CO_3^{--} concentration were monitored and recorded simultaneously. After the system returned to a steady state, a sample of the outlet liquid was taken again to check the uniformity of sodium hydroxide concentration.

The pulse tests were made on two packing materials, ¼-in. Raschig rings and ¾-in. Berl saddles. Sets of data were obtained for nominal gas flow rates of 2, 5, and 10 lb.-moles/hr./sq.ft. at each of 4 liquid flow rates, 25, 50, 100, and 200 lb.-moles/hr./sq.ft. and at zero liquid flow over dry packing.

RESULTS AND DISCUSSION

Treatment of Data

A typical set of recorded experimental pulse response curves (inlet gas, outlet gas, and outlet liquid compositions versus time) are shown in Figure 2. The corresponding frequency responses (Bode plots) are presented in Figures 3a and 3b. The maximum depletion of hydroxyl ion in this example is 8.5% and for the other runs the maximum hydroxyl ion conversion was normally less than 10%, satisfying the assumption of constant β in the theoretical analysis.

In this connection, it can be shown mathematically using the slug flow model that the maximum hydroxyl ion depletion in the liquid phase occurs at the liquid outlet end (bottom) of the column, that is, the point of measurement in this study. This can also be arrived at intuitively, since the peak in the liquid composition-time pulse, representing peak hydroxyl ion depletion, could decrease toward the liquid outlet end of the column *only* if carbon dioxide were leaving the liquid phase. For irreversible absorption this would not occur, and the peak must increase reaching its maximum at the liquid outlet.

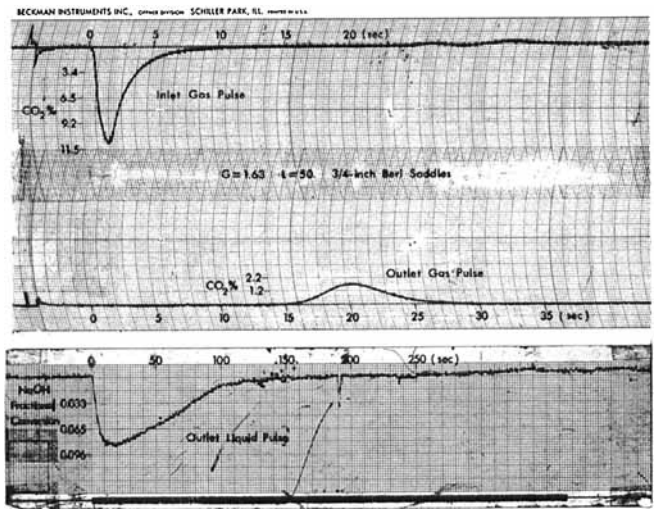

Fig. 2. Typical recorded experimental pulses.

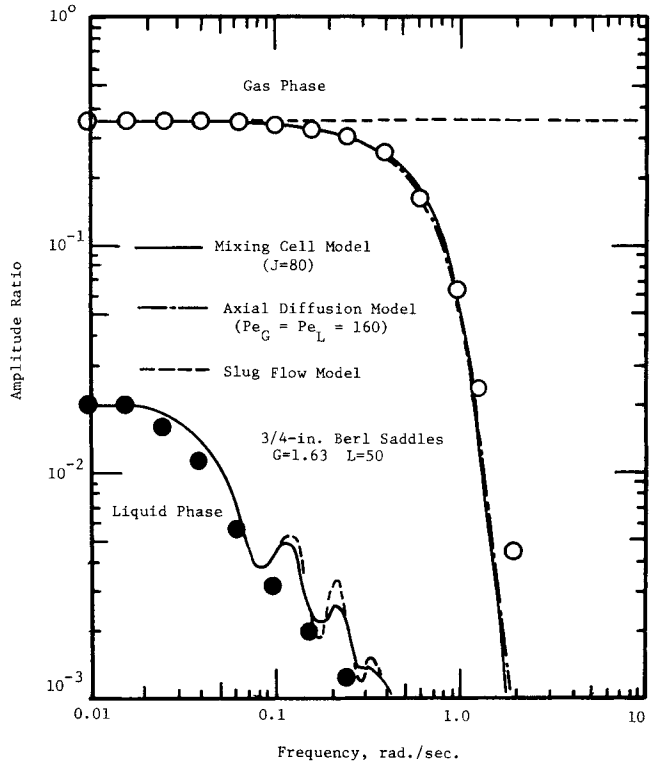

Fig. 3a. Comparison of theoretical frequency response amplitude ratios of slug flow, mixing cell, and axial diffusion models.

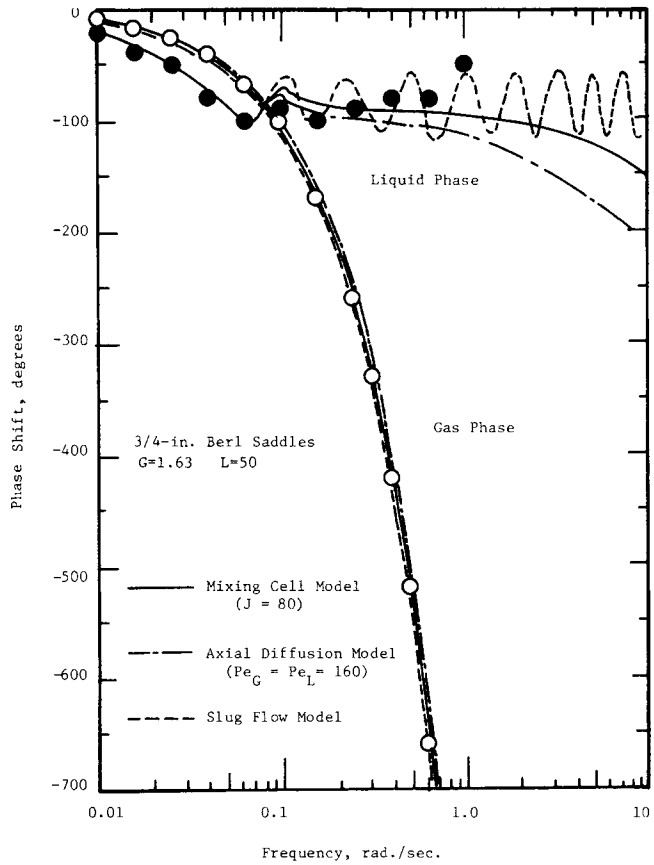

Fig. 3b. Comparison of theoretical frequency response phase shifts of slug flow, mixing cell and axial diffusion models.

Experimental pulse response data were reduced to frequency response by Fourier analysis after corrections for imperfect material balance were made. The material balance correction was necessitated by slow drift in the calibration of the electrical conductivity cells and the sensitivity of material balance calculations to small liquid composition errors (due to high liquid/gas flow rate ratios). In each run, the electrical conductivity cell calibration was adjusted to force closure of the carbon dioxide material balance for the column. The correction in no way changed the shape of the Bode plot curves, merely adjusting the vertical position of the liquid-phase amplitude ratio curves.

Dynamic responses obtained from the experimental pulses were considered to represent the response of the column packed section only. This was believed to be a reasonable assumption because pulses were monitored just when they entered or left the packed section, essentially eliminating end-section effects, and both the inlet and outlet thermal conductivity cells had the same dynamic characteristics, thus cancelling out their effect on the overall response. Although the electrical conductance cell had different dynamic characteristics from the thermal conductivity cells, the difference was ignored in the calculation of the liquid-phase dynamic response since the dynamic response of the liquid phase was much slower than that of either the thermal conductivity cells or electrical conductance cell.

The parameters necessary to calculate the theoretical frequency responses were obtained as follows. The number of transfer units N was determined from the experimental gas-phase amplitude ratio at zero frequency assuming that the slug flow model Equation (6) held at this frequency. (The axial diffusion and mixing cell models gave zero-frequency predictions identical with this equation.) The gas-phase residence time θ_G was calculated from the holdup and flow rate measurements. This θ_G was compared with the residence time determined by measuring the time length between the recorded peaks of inlet and outlet gas pulses, and the difference was found to be very small. The liquid-phase residence time was calculated from the results of liquid holdup and void fraction measurements.

Frequency Content

A problem in applying the pulse response technique is to produce an input pulse with sufficient frequency content. The maximum frequency at which information can be obtained is that above which the input or output amplitude decreases below the noise level of the system. After this point the experimental amplitude ratios and phase shifts show erratic behavior indicating that data reduction for higher frequency will be meaningless. Reliable data were obtained over the frequency range 0 to 5 radians/second.

Comparison of Models

Three theoretical frequency responses based on the slug flow model, mixing cell model, and axial diffusion model are compared with experimentally obtained frequency responses in Figure 3. Theoretical results are shown by solid and dashed curves and experimental results are shown as a series of points.

The agreement between the experimental gas-phase amplitude ratios and the theoretical predictions of the mixing cell or the axial diffusion model is excellent up to the maximum frequencies. The parameters, number of cells and Peclet number, were chosen by trial to fit the experimental data. Above the maximum frequency, the experimentally determined amplitude ratios deviated from the theoretical predictions and are not shown in the figures. The slug flow model fails to predict the gas-phase experimental amplitude ratio after the frequency at which the amplitude ratio starts to fall off. The slug flow model does not predict an increasing attenuation of gas-phase amplitude ratio with increasing frequency. This is easily seen from Equation (6), the slug flow model gas-phase transfer function, since it simply represents a constant attenuation and a time delay.

It should be emphasized that these results do not apply for the case of reversible absorption, that is, purely physical absorption or absorption accompanied by reversible chemical reaction. In such cases the duration of outlet gas and liquid pulses will usually be significantly greater than in the irreversible case, due to repeated desorption and resorption of the solute gas. For reversible absorption, the slug flow model predicts gas-phase amplitude ratio curves that exhibit an attenuation and then approach a constant asymptote as frequency increases (9); the gas-phase amplitude ratio curves for mixing cell and axial diffusion models exhibit first an attenuation, then a plateau-like leveling off, and finally further attenuation, as frequency is increased (3).

The agreement of liquid-phase amplitude ratio between the experiments and theories is very good, except that the theoretical predictions show oscillations as they decrease from the constant values at low frequencies. The mixing cell model and the axial diffusion model predictions are identical within the range of the scale of the figures, and the slug flow model prediction is almost identical to them except that it exhibits a larger degree of oscillation.

For the gas-phase phase shifts the agreement between the experimental results and the theoretical predictions is excellent. The predictions from the three models coincide.

Experimental phase shifts for the liquid phase are well predicted by the three models. Deviation of the experimental results from the theoretical predictions starts above the maximum frequency. The curve for the slug flow model oscillates considerably as frequency increases, while those for the mixing cell model and axial diffusion model do not. The three models give very similar predictions for lower frequencies, but they diverge as frequency increases.

Number of Cells and Peclet Number

The similarity of the mixing cell model and axial diffusion model for long beds has been demonstrated from theoretical considerations by Kramers and Alberda (*12*) and Aris and Amundson (*1*). They obtained the following relationship for the number of cells in the mixing cell model and Peclet number in the axial diffusion model by assuming the column to act as a series of perfectly mixed cells with height of γd_p, where d_p is packing diameter and γ is a constant (greater than 1.0 in general):

$$Pe = \frac{Ud_p}{E}\frac{Z}{d_p} = \frac{2}{\gamma}\frac{Z}{d_p} = 2\frac{Z}{\Delta z} = 2J. \qquad (18)$$

They assumed that γ approached 1.0 as packing Reynolds number increased. This has been demonstrated experimentally by McHenry and Wilhelm (*13*) for single-phase gas flow in packed beds.

The effect on calculated frequency response of the choice of theoretical parameters is illustrated in Figure 4 for three sets of number of cells and Peclet number under the relation of Equation (18). The two models do not give identical curves but very similar ones. Break points occur at higher frequency as the number of cells or Peclet number increases, thus indicating an approach to the slug flow behavior. For the liquid-phase amplitude ratio, the two models give almost exactly the same predictions for

a given set of parameters, as shown by a single curve. The degree of oscillation becomes larger and approaches that of the slug flow model as the number of cells or Peclet number increases.

Indistinguishable gas-phase phase shifts are exhibited by the two models independent of the parameters. This is in agreement with the preceding result that the slug flow model, which can be considered as a mixing cell model with an infinite number of cells or an axial diffusion model with an infinite Peclet number, gave almost the same predictions as the mixing cell or the axial diffusion model. This indicates that the phase shifts are primarily determined by the gas-phase transit time through the packing. That the phase angle approximation for the axial diffusion model is identical to the exact relationship for the slug flow model has been shown theoretically by Gray and Prados (9) for their single-phase flow experiment. Therefore, conclusions concerning the agreement for the gas phase between theory and experiment should be based primarily on amplitude ratio data.

For the liquid-phase phase shift, the two models give identical predictions for lower frequencies and then diverge as frequency increases. For higher frequencies the absolute phase shift calculated by the axial diffusion model is larger than that for the mixing cell model, and the difference, although small, increases as the mixing parameters decrease. As the parameters become larger, the magnitude of oscillation at lower frequency becomes larger and the curves decline less after the divergence of the curves.

The number of mixing cells or Peclet number which provide the best description of experimental data were determined by trial and error. In general, a number of cells (J) near 150 (or Peclet number around 300) appeared to be the optimum values to predict the gas-phase amplitude ratio for the experiments with ¼-in. Raschig rings, and a value of J near 80 (or Pe around 160) appeared to be optimum for the ¾-in. Berl saddle experiment. However, changes of 10 to 20% in the number of cells or Peclet number did not appreciably change the calculated frequency responses as can be observed in the figure.

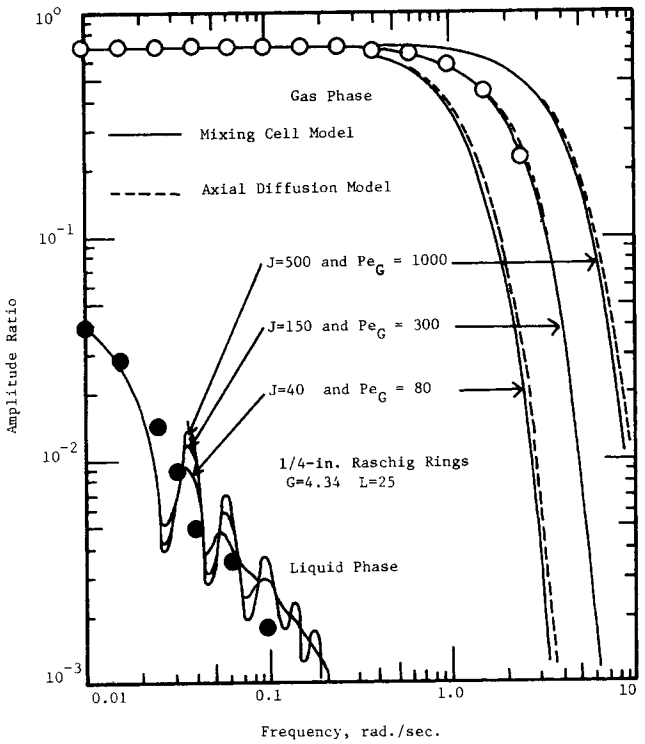

Fig. 4a. Effect of number of cells and Peclet number on amplitude ratios.

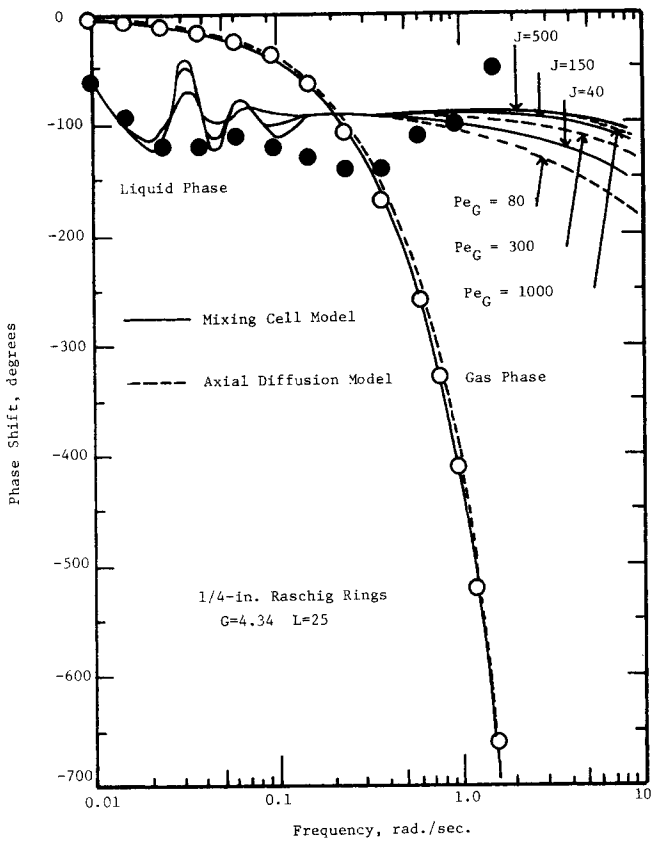

Fig. 4b. Effect of number of cells and Peclet number on phase shifts.

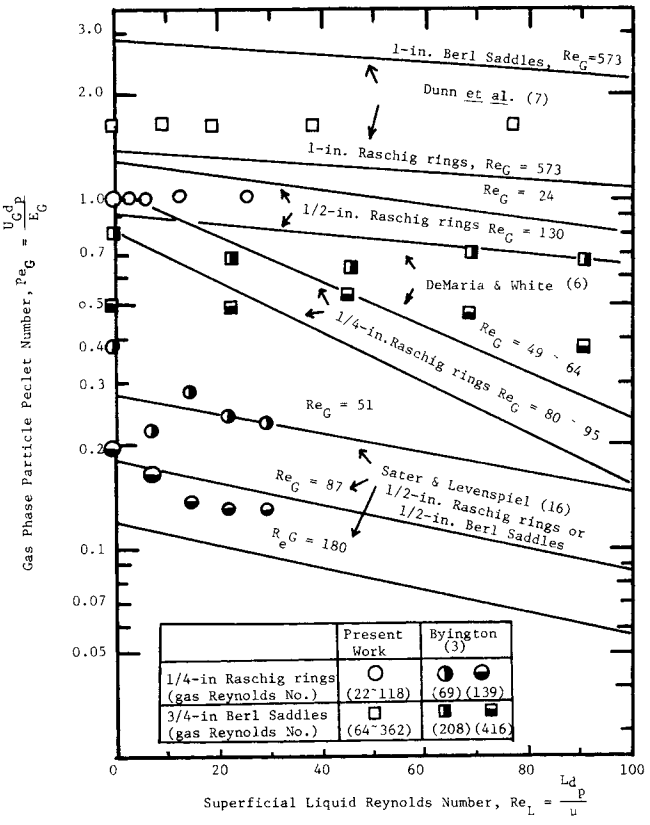

Fig. 5. Comparison of gas-phase particle Peclet number with literature values.

A number of experimental investigations have been made to determine the nature and magnitude of axial diffusion for single-phase and two-phase flows through packed beds (*3, 6, 7, 16*). A graphical comparison of the present result on gas-phase mixing with results reported in the literature employing the same or similar types of packing is made in Figure 5. As can be seen, gas-phase particle Peclet numbers in the present work were in reasonable agreement with the literature data which themselves are quite scattered.

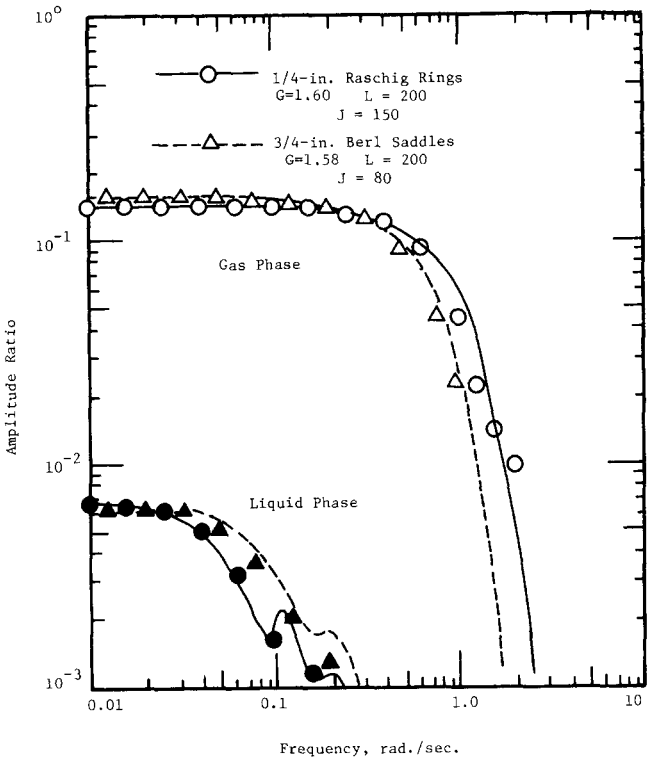

Fig. 6a. Effect of packing characteristics on amplitude ratios.

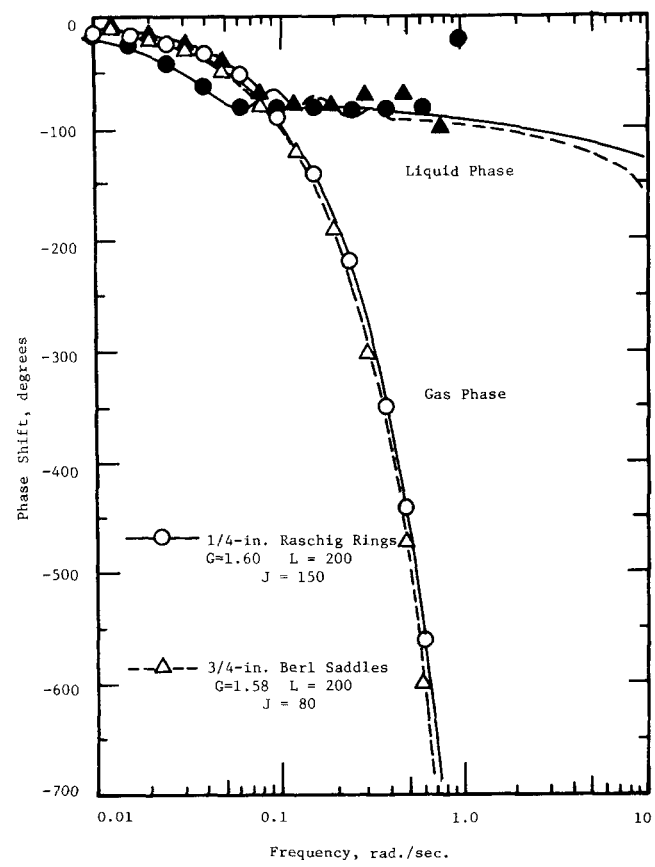

Fig. 6b. Effect of packing characteristics on phase shifts.

Since the mixing cell model provides an easier mathematical approach for unsteady state application than does the axial diffusion model (9), the two models give very similar frequency responses as described above, and the slug flow model obviously fails to predict gas-phase amplitude ratios, only the mixing cell model will be used to present the theoretical curves for comparison in the subsequent figures.

Effect of Packing Characteristics

The effect of packing characteristics on the packed column dynamic response is demonstrated by comparing the results between the two packings obtained at the same operating conditions, that is, at the same nominal gas and liquid flow rates. The two packings, ¼-in. Raschig rings and ¾-in. Berl saddles, possess considerably different liquid holdup characteristics. Typical results with very low gas and very high liquid flow rates are presented in Figure 6. No effects are seen in the sense that the experimentally obtained frequency responses are all very well described by the model without regard to the packing characteristics. It is, of course, understood that the difference between the two curves in the figure resulted from the difference in the experimental operating parameters, mass transfer coefficients, fluid transit times, and degree of mixing of fluids.

Effect of Gas Flow Rate

The effect of the gas flow rate on the frequency response is studied by varying the nominal gas flow rates while other operating conditions are maintained the same. The results are shown in Figure 7. No effect of gas rate is evident in that the experimentally obtained frequency responses are well predicted by the mixing cell model regardless of the gas flow rate. The vertical position of the three gas amplitude ratio curves for low frequencies is determined primarily by the parameter N, the number of transfer units, which is related to the gas flow rate and mass transfer coefficient. The larger the value of N the greater the attenuation at low frequencies, as can be easily seen from Equation (6) for the slug flow model.

For gas-phase amplitude ratio and phase shift, the relative shift of the three curves with respect to frequency is produced by the differences in the gas transit time which is inversely proportional to the gas flow rate. It is of interest to note therefore that the three curves for the gas phase will coincide if the dimensionless frequency parameter $\Omega = \omega\theta_G$ is used instead of ω and if the numbers of transfer units are equal. This is easily seen from Equations (10) and (11), and is demonstrated in Figure 8 for dry packing for which N is zero. The experimental data lie well on the single theoretical curve.

Effect of Liquid Flow Rate

The effect of liquid flow rate was studied by examining the frequency response curves obtained at different liquid flow rates. The results are shown in Figure 9. Vertical shifts of the gas-phase amplitude ratio at low frequencies are clearly seen. This is caused by a change in number of transfer units as determined by the mass transfer coefficient K_Ga for constant gas flow rates. Horizontal shifts of the gas-phase amplitude ratio and the phase shift curves with liquid flow rate changes are hardly seen. Their horizontal positions are primarily determined by gas-phase transit

time, and this is essentially independent of liquid flow rate except near flooding conditions.

Mass Transfer Coefficient

The overall mass transfer coefficients K_Ga based on gas-phase driving force were calculated from the number of transfer units. The results are presented as a plot of K_Ga versus liquid flow rate in Figure 10. The literature values reported by Blum et al. (*2*) and Onda et al. (*14*) for their steady state experiments with sodium hydroxide solutions of approximately the same concentration as those used in the present experiment are also plotted for comparison. Since their K_Ga's were obtained at average liquid

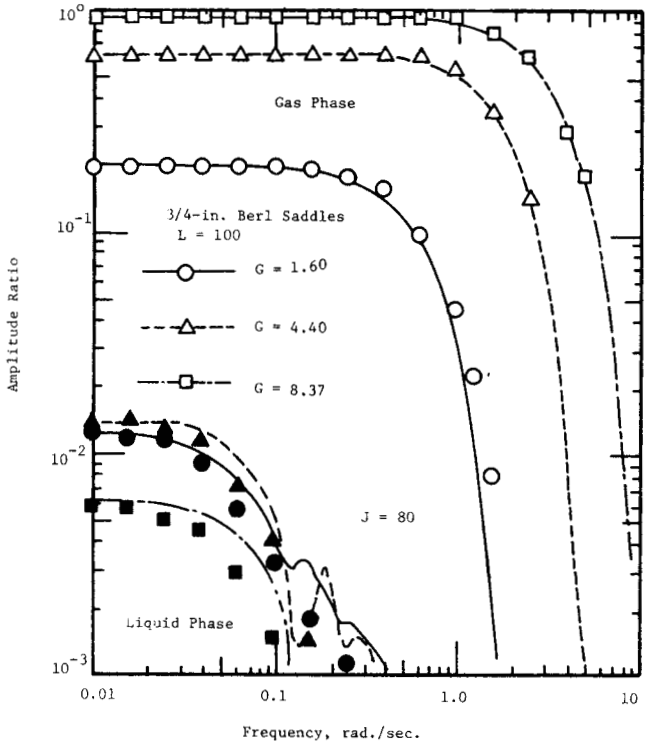

Fig. 7a. Effect of gas flow rate on amplitude ratios.

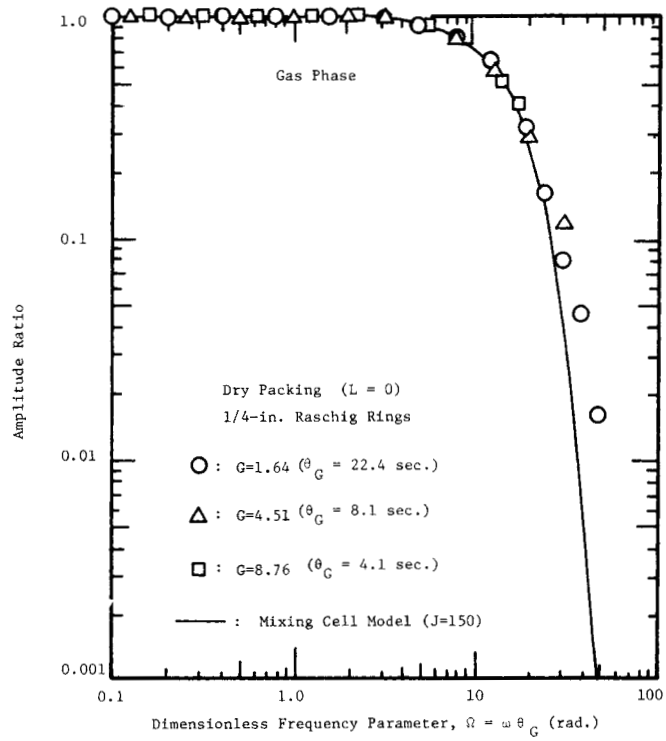

Fig. 8a. Amplitude ratio versus dimensionless frequency parameter.

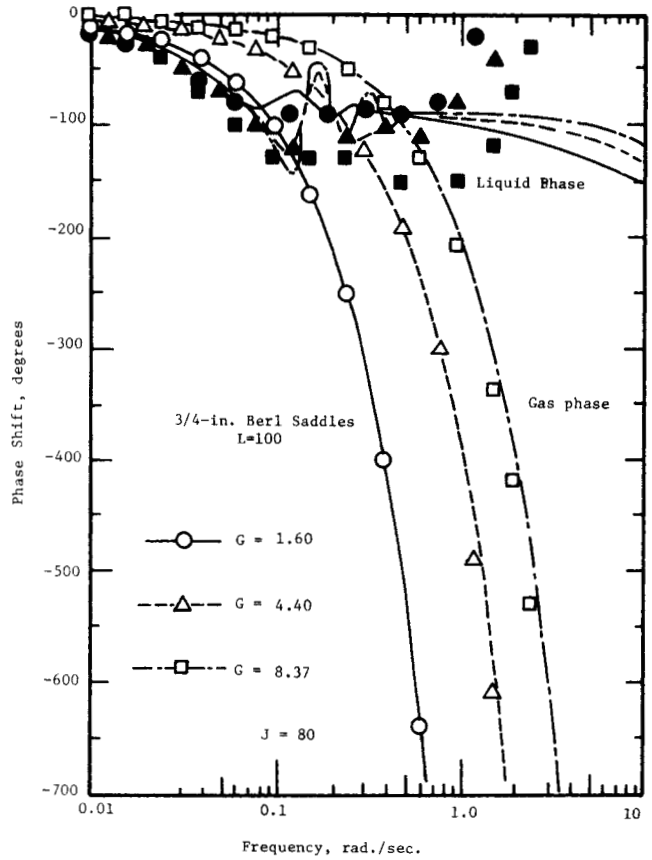

Fig. 7b. Effect of gas flow rate on phase shifts.

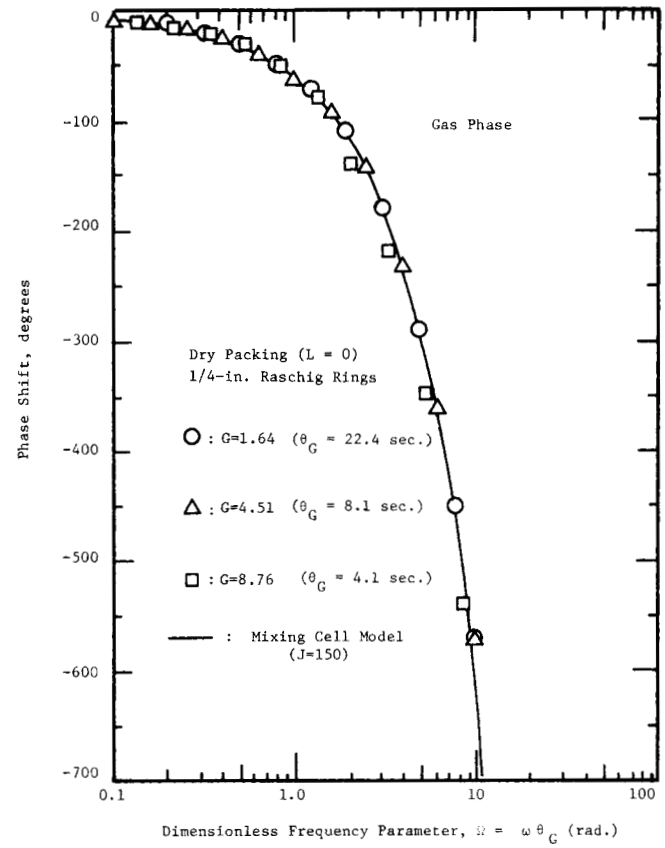

Fig. 8b. Phase shift versus dimensionless frequency parameter.

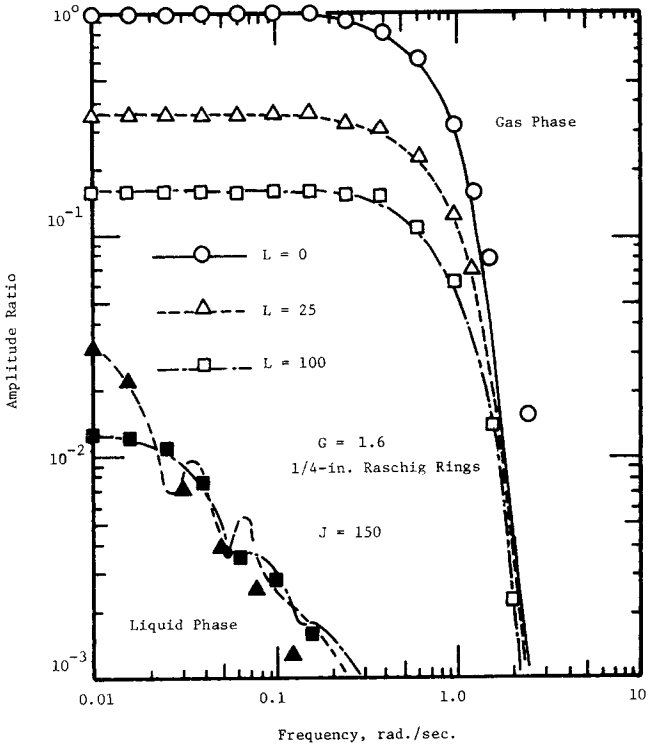

Fig. 9a. Effect of liquid flow rate on amplitude ratios.

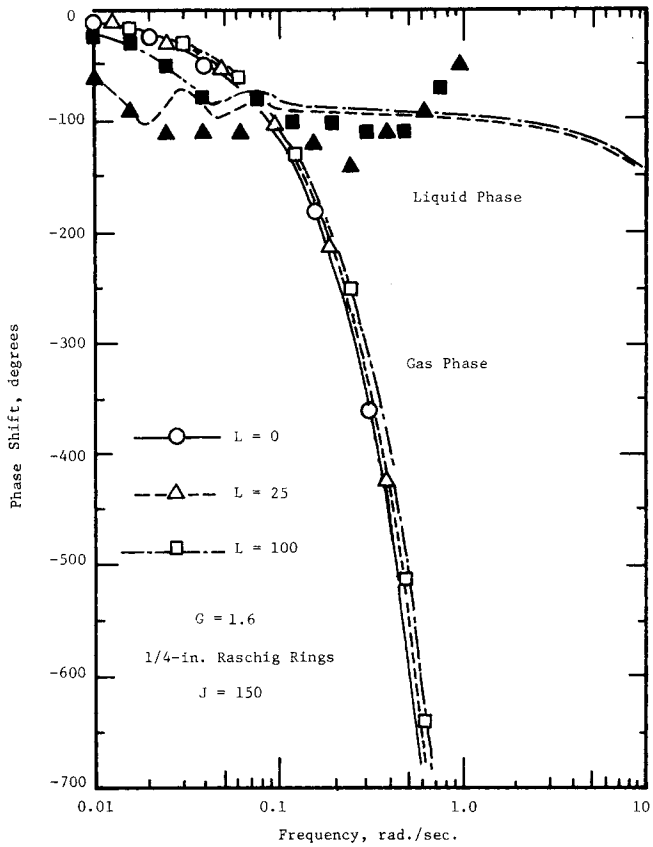

Fig. 9b. Effect of liquid flow rate on phase shifts.

temperatures of 27°C. and 30°C. respectively, corrections for temperature effect were made to estimate their K_Ga's at the present average liquid temperature 15°C. The correlation that K_Ga varies as approximately the sixth power of absolute liquid temperature obtained by Tepe and Dodge (*17*) was used. The agreement of K_Ga values between the present work and the literature is fairly good although different packings were employed [no noticeable effect of packing size on K_Ga has been observed by Blum et al. (*2*)].

CONCLUSIONS

An investigation on the dynamics of a packed column for absorption with chemical reaction by the pulse response technique was conducted. The following conclusions are drawn from the results of the investigation.

1. Both the mixing cell model and the axial diffusion model adequately predict the experimental gas-phase amplitude ratios up to the maximum frequency at which data can be obtained. The slug flow model is not successful at the higher frequencies where axial mixing affects the amplitude ratios.
2. The three models give indistinguishable and excellent predictions of the experimental gas-phase phase shift. The phase shift is primarily determined by gas-phase transit time.
3. Experimental liquid-phase amplitude ratios are well described by any one of the three models. The three models give essentially the same predictions.
4. Liquid-phase phase shift data agree with any one of the three models up to the maximum frequency. The three models show very similar predictions at low frequencies and then they diverge as frequency increases, with considerable oscillation for the slug flow model.
5. Frequency responses for the present absorption system are determined by the following major parameters: the number of transfer units which incorporates a mass transfer coefficient, the ratio of phase flows (slope of operating line), the Peclet number or number of mixing cells, and the dimensionless frequency parameter associated with phase transit times.

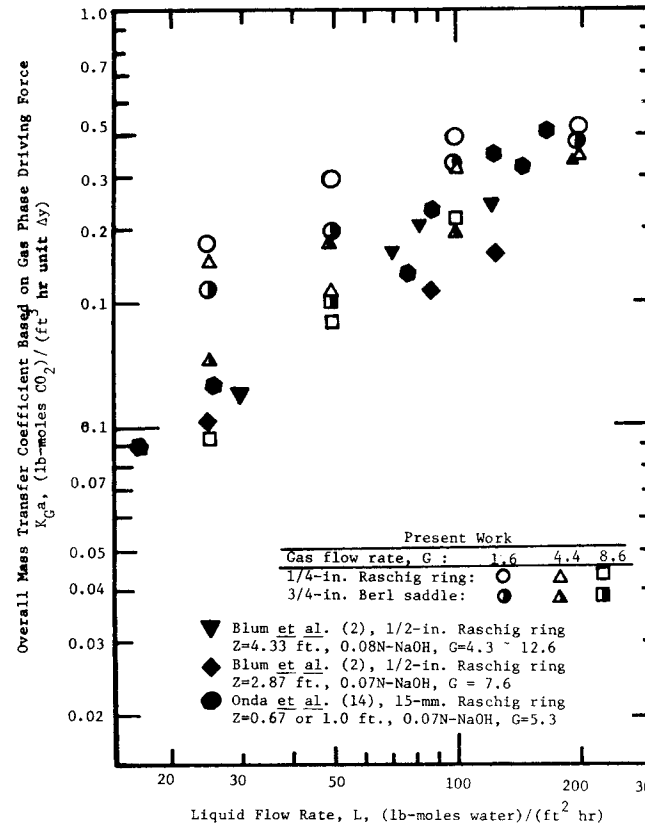

Fig. 10. Mass transfer coefficients versus liquid flow rate.

6. Gas-phase particle Peclet numbers determined in the present work were in reasonable agreement with the values reported in literature.

7. Overall mass transfer coefficients based on gas-phase driving force determined from the present absorption system were in fair agreement with the values reported in literature.

NOTATION

a = mass transfer area, sq.ft./cu.ft.
C_{OH^-} = average concentration of OH^-, lb.-moles/cu.ft.
d_p = nominal size of packing, ft.
D_{CO_2} = diffusivity of carbon dioxide in liquid, sq.ft./hr.
E_G, E_L = axial eddy diffusivity, sq.ft./hr.
G = gas flow rate, lb.-moles/hr./sq.ft.
h_G, h_L = holdup, lb.-moles/cu.ft.
i = $\sqrt{-1}$, imaginary unit
j = designation for a mixing cell increment
J = number of mixing cells in column
k = reaction rate constant, cu.ft./lb.-moles/hr.
k_G, k_L = mass transfer coefficient, lb.-moles/hr./sq.ft./mole fraction
K_Ga = overall mass transfer coefficient based on gas-phase driving force, lb.-moles/hr./sq.ft./mole fraction
L = liquid flow rate, lb.-moles/hr./sq.ft.
m = slope of gas-liquid equilibrium line, mole fraction in gas/mole fraction in liquid
N = K_GaZ/G, total number of transfer units in column
p = parameter defined by Equation (12)
pe_G, pe_L = Ud_p/E, particle Peclet number
Pe_G = ZG/E_Gh_G, column Peclet number for gas phase
Pe_L = ZL/E_Lh_L, column Peclet number for liquid phase
q = parameter defined by Equation (12)
Ra = mass transfer rate, lb.-moles/hr./cu.ft.
s = Laplace transform parameter, 1/time
t = time, sec. or hr.
U = interstitial velocity, ft./hr.
x = mole fraction of solute in liquid phase
x_j = liquid phase composition in jth mixing cell
x_{J+1}, x_Z = solute mole fraction in liquid entering column
x_0 = solute mole fraction in liquid leaving column
y = mole fraction of solute in gas phase
y_j = gas phase composition in jth mixing cell
y_J, y_Z = solute mole fraction in gas leaving column
y_0 = solute mole fraction in gas entering column
z = longitudinal distance from base of packing, ft.
Z = height of packing, ft.

Greek Letters

β = $\Gamma/\tanh\Gamma$ = reaction factor
Γ = $\sqrt{k\,C_{OH^-}\,D_{CO_2}}/k_L$
γ = constant used in Equation (18)
Δz = height of one mixing cell, ft.
θ_G = h_GZ/G, column gas-phase transit time, sec. or hr.
θ_L = h_LZ/L, column liquid-phase transit time, sec. or hr.
θ_T = $\theta_G + \theta_L$
μ = viscosity, lb./hr./ft.
ϕ = L/G, ratio of flow rates
ω = frequency, rad./sec.
Ω = $\omega\theta_G$, dimensionless frequency parameter
G = gas phase
L = liquid phase
$\bar{}$ = Laplace transform of variable

Grouped Coefficients

$$A = \frac{1}{m_1 - n_1} + \frac{1}{m_1 - n_2}$$

$$B = \frac{1}{m_2 - n_1} + \frac{1}{m_2 - n_2}$$

$$b_1 = \frac{m_2 Pe_G}{m_2^2 - m_1^2\, e^{m_1 - m_2}}$$

$$b_2 = \frac{m_1 Pe_G}{m_1^2 - m_2^2\, e^{m_2 - m_1}}$$

$$c_2 = \frac{Ab_1[m_1n_2\, e^{n_1} + n_1(Pe_L + m_1)e^{m_1}] + Bb_2[m_2n_2\, e^{n_1} + n_1(Pe_L + m_2)e^{m_2}]}{n_1^2\, e^{n_2} - n_2^2\, e^{n_1}}$$

$$c_1 = \frac{Ab_1[m_1n_1\, e^{n_2} + n_2(Pe_L + m_1)e^{m_1}] + Bb_2[m_2n_1\, e^{n_2} + n_2(Pe_L + m_2)e^{m_2}]}{n_1^2\, e^{n_2} - n_2^2\, e^{n_1}}$$

$$m_1,\, m_2 = \frac{Pe_G \pm \sqrt{Pe_G^2 + 4Pe_G(N + \theta_G s)}}{2}$$

(m_1 requiring the positive sign)

$$n_1,\, n_2 = \frac{-Pe_L \pm \sqrt{Pe_L^2 + 4Pe_L\,\theta_L\, s}}{2}$$

(n_1 requiring the positive sign)

LITERATURE CITED

1. Aris, R., and N. R. Amundson, *AIChE J.*, 3, 280 (1957)
2. Blum, H. A., L. F. Stutzman, and W. S. Dodds, *Ind. Eng. Chem.*, 44, 2969 (1952).
3. Byington, J. A., Ph.D. dissertation, Univ. of Tennessee, Knoxville (1969).
4. Clements, W. C., and K. B. Schnelle, *Ind. Eng. Chem. Process Design Develop.*, 2, 94 (1963).
5. Danckwerts, P. V., *Chem. Eng. Sci.*, 2, 1 (1953).
6. Demaria, F., and R. R. White, *AIChE J.*, 6, 473 (1960).
7. Dun, W. E., T. Vermeulen, C. R. Wilke, and T. T. Word, Report 10394, Univ. California Radiation Lab., Berkeley (1963).
8. Fan, L. T., and Y. K. Ahn, *Chem. Eng. Prog., Proc. Systems Eng.*, 59, 91 (1963).
9. Gray, R. I., and J. W. Prados, *AIChE J.*, 9, 211 (1963).
10. Hatta, S., *Tech. Repts.*, Tohoku Imp. Univ., 10, 119 (1932).
11. Hougen, J. O., and R. A. Walsh, *Chem. Eng. Progr., Process Dynamics Control*, 57, 69 (1961).
12. Kramers, H., and G. Alberda, *Chem. Eng. Sci.*, 2, 173 (1953).
13. McHenry, K. W., Jr., and R. H. Wilhelm, *AIChE J.*, 3, 63 (1957).
14. Onda, K., E. Sada, and H. Takeuchi, *J. Chem. Eng. Japan*, 1, 69 (1968).
15. Sakata, N., M.S. thesis, Univ. Tennessee, Knoxville (1968).
16. Sater, V. E., and O. Levenspiel, *Ind. Eng. Chem. Fundamentals*, 5, 86 (1966).
17. Tepe, J. B., and B. F. Dodge, *Trans. Am. Inst. Chem. Engrs.*, 39, 255 (1943).

Manuscript received June 14, 1971; revision received December 21, 1971; paper accepted December 22, 1971.